Quantum sensing of ultralow temperature in biwire ultracold polar molecules

Abdelâali Boudjemâa [1,*] Karima Abbas [1] Asma Tahar Taiba,[2] and Qing-Shou Tan [3]

[1]*Department of Physics, Faculty of Exact Sciences and Informatics and Laboratory of Mechanics and Energy, Hassiba Benbouali University of Chlef, P.O. Box 78, 02000, Chlef, Algeria*

[2]*LPTHIRM, Department of Physics, Faculty of Sciences, University of Blida 1, P.O. Box. 270, 09000, Blida, Algeria*

[3]*Key Laboratory of Hunan Province on Information Photonics and Freespace Optical Communication, College of Physics and Electronics, Hunan Institute of Science and Technology, Yueyang 414000, China*

(Received 7 May 2024; accepted 29 August 2024; published 12 September 2024)

We present a systematic study of quantum sensing of ultralow temperature in biwire ultracold polar molecules of a quasi-one-dimensional (1D) trap by exploring the dynamics of two physically different qubit models. The two models consist of a trapped impurity atom that act as a temperature quantum sensor interacting with polar molecules reservoir, where dipole moments are aligned head-to-tail across the wires. Our model takes advantage of the adjustable interwire distance to accurately control the precision ultralow temperatures measurement. We show that the system undergoes a transition from Markovian to non-Markovian dynamics, which can be controlled by changing the interwire separation, the dipole—dipole interaction (DDI), and the temperature. We characterize the thermometric performance using the quantum signal-to-noise ratio for both models and demonstrate that such a quantity exhibits a higher peak at ultralow temperature. We therefore emphasize that ultracold polar molecules are crucial for revolutionizing temperature sensing.

DOI: 10.1103/PhysRevA.110.032611

I. INTRODUCTION

A high-precision ultralow temperatures measurement is crucial not only for quantum physics but also for multiple quantum technologies such as quantum sensing [1–3], quantum information processing [4], and quantum many-body simulations [5,6].

The achievement of laser and evaporative cooling techniques made it possible to attain temperatures in the nK and sub-nK regime [7–10]. The most prominent success of these methods is the observation of a Bose-Einstein condensate (BEC) [11,12], a quantum degenerate Fermi gas [13], a dipolar BEC [14] in dilute quantum atomic gases, and an ultracold gas of polar molecules [15,16].

The temperature of an ultracold gas, which is commonly measured using an absorption imaging in the nK regime [17], is inferred from its density, i.e., the sensing error in the measurement of temperatures substantially grows at very low temperatures [10]. So far, several schemes to enhance the quantum sensitivity of the temperature of both dipolar and nondipolar BECs have been introduced [18–29]. However, achieving nondestructive ultralow temperature measurements still presents challenges.

Recently, quantum sensing of temperature near the absolute zero, i.e., quantum thermometry, has attracted a great deal of interest [18–31]. A perfect thermometer should be small enough in such a way its coupling with its host should not affect the measurement of its temperature. The theoretical design of the smallest quantum thermometer that can measure extremely small changes in temperature is based on small quantum systems, serving as probes, such as a two-level system [5,32–40] or a harmonic oscillator [41–43]. These probes interact with a thermal bath and encode temperature information into their quantum states. Temperature is extracted from observables of the probe system. The exploitation of quantum entanglement, quantum coherence, quantum non-Markovian, and other quantum features in such quantum temperature sensors has great potential to outperform temperature measurement techniques based on classical physics [3,44].

In this paper, we theoretically propose a quantum thermometer based on the measurement of a mixed bosonic system consisting of an impurity qubit in contact with a thermal bath made up of one-dimensional (1D) biwire (tube) ultracold polar molecules. It is worth stressing that such a thermometer prototype remains widely unexplored. The realization of a quantum degenerate gas of polar molecules [15,16] which establishes a long-range and anisotropic interaction among molecules, offer a unique setting for sensing the temperature with high precision and a negligible disturbance of the bath. Polar molecules may be better suited than neutral atoms for boosting the accuracy of temperature measurements, as they possess tunable electric dipole moment which can be induced by a static dc electric field, in addition to their own intrinsic dipole moment [15,16]. Recent studies

*Contact author: a.boudjemaa@univ-chlef.dz

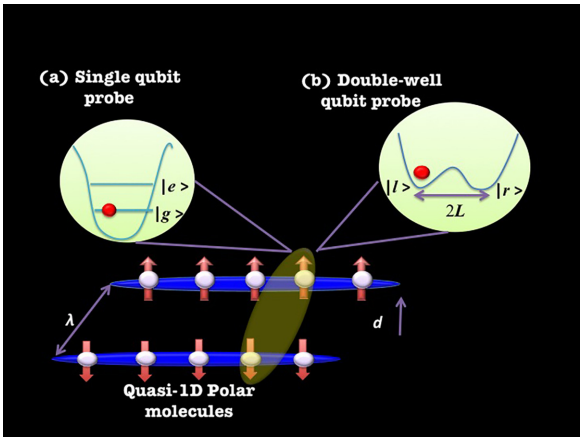

FIG. 1. (a) A single impurity atom, with an internal level structure, trap in a deep harmonic trap. (b) An atomic qubit trapped in a double-well potential, the distance between two wells in the same trap is $2L$. Each qubit interacts with a thermally equilibrated quasi-1D biwire system of cold polar molecules with dipoles oriented in opposite directions in different wires. Here the impurity qubit atom acts as a quantum sensor to estimate the temperature of the molecules.

have shown that unconventional d- and f-wave superfluids of fermionic polar molecules in a two-dimensional (2D) bilayer geometry occur at temperatures well below any temperature that has been reached so far (i.e., pK and fK regimes) [45,46].

The aim is to investigate the dynamics of two different qubit models, namely, the following: (i) single-qubit probe and (ii) double-well qubit probe that act as the sensor, dephasing under the effect of a thermally equilibrated 1D biwire ultracold polar molecules reservoir. Such a biwire configuration constitutes an ideal platform to investigate the properties of polar molecules since it allows for stability against chemical reactions and includes an additional controllable parameter, interwire space, which leads to boosting the controllability of the system at hand. The dipole moments are assumed to be aligned perpendicularly to the tubes by an external field and in opposite directions in different wires (see Fig. 1). The interaction of the impurity qubit with its polar molecules environment is described within the realm of the exact pure dephasing model (known also as a spin-boson model) [19]. A transition from Markovian to non-Markovian dynamics is observed here through variation of the interwire separation and the temperature. However, such a non-Markovianity measure decreases with the dipole-dipole interaction (DDI) for both models in agreement with the results of Ref. [29].

Furthermore, we numerically investigate the temperature-sensing performance using the quantum signal-to-noise ratio (QSNR) in terms of the interwire space and the DDI strength for both models. We discover that the QSNR attains its maximum at a certain optimal encoding time which is inversely proportional to temperature and to interwire distance. On the other hand, we show that the coupling of the qubit to collective excitations of the reservoir which develops a roton-maxon structure may significantly decohere the qubit and thus, holds the promise of inducing strong non-Markovian effects. It is also found that such a rotonization modifies the QSNR and the thermometric performance of our models.

The rest of the paper is organized as follows. Section II introduces the two models of impurity qubit immersed in a thermally equilibrated quasi-1D polar molecules reservoir. We describe the dynamics and the non-Markovianity measure of such qubit models under the influence of the dephasing noise. The temperature sensing protocol is also briefly discussed. Section III is devoted to numerical simulations. We look, in particular, at how the interwire space, the temperature and the DDI affect the non-Markovianity, the QSNR, the maximum achievable QSNR, and the temperature optimal relative error of both models. Finally, our conclusions and discussions are drawn in Sec. V.

II. MODELS

We consider dipolar BECs loaded in a biwire system of a quasi-1D trap, where the two wires are separated by a distance λ, assuming a vanishing hopping between wires. The dipole moments are assumed to be aligned perpendicularly to the tubes by an external field and in opposite directions in different wires. Here we investigate the dynamics of two different qubit models that act as the sensor, each embedded in a thermally equilibrated ultracold polar molecules reservoir at temperature T. In model I, the impurity is trapped in a deep harmonic trap and has two internal levels, $|e\rangle$ and $|g\rangle$ representing the qubit states [47] [see Fig. 1(a)]. In model II, the atomic qubit is trapped in a double-well potential and forms an effective qubit system where the two qubit states are represented by occupation of the impurity in the left $|l\rangle$ or the right $|r\rangle$ [19] [see Fig. 1(b)].

For model I, we suppose that the impurity qubit with two hyperfine spin states is confined in a harmonic trap $U_I(\mathbf{r}) = m_I\omega_I^2 r^2/2$ that is independent of the internal states, where m_I is the mass of the impurity and ω_I is the trap frequency. For $\hbar\omega_I \gg 1$, the spatial wave function of the qubit is given by $\psi_I = \pi^{-3/4}\mathfrak{l}_I^{-3/2}\exp(-r^2/2l_I^2)$, where $l_I = \sqrt{\hbar/m_I\omega_I}$ is the impurity harmonic oscillator length. The Hamiltonian of the sensor is given by [48]

$$H_I^{\text{model I}} = \frac{\hbar\Omega}{2}(|e\rangle\langle e| - |g\rangle\langle g|), \tag{1}$$

where Ω is the level splitting between the excited $|e\rangle$ and ground $|g\rangle$ states.

Now for model II, we assume an impurity atom in the double-well system where the distance between two wells in the same trap is $2L$. Therefore, the Hamiltonian of the sensor can be written in terms of the Pauli operators $\sigma_z = |l\rangle\langle l| - |r\rangle\langle r|$ as

$$H_I^{\text{model II}} = \frac{\hbar}{2}[\Omega_r(1+\sigma_z) + \Omega_l(1-\sigma_z)], \tag{2}$$

where $\hbar\Omega_{l,r}$ are the energies of the impurity.

Regarding the polar molecules (reservoir) with mass m and dipole moment d placed in two wires, we assume that they are harmonically confined in a quasi-1D geometry with the axial trap frequency ω_x being much smaller than the radial trap frequency $\omega_\perp$. The interaction potential has a contact component related to the s-wave scattering length a as $V_c(x) = g_{1D}\delta(x) =$

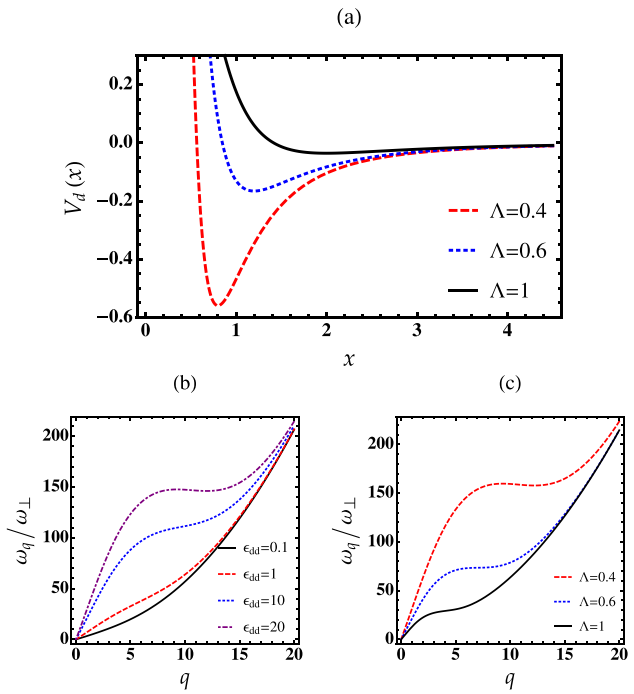

FIG. 2. (a) Interwire interaction potential as a function of x for different values of the interwire distance and $g_d = 1$. (b) The Bogoliubov spectrum from Eq. (5) for different values of $\epsilon_{\rm dd}$ with $\alpha = 4.5$ and $\Lambda = 0.4$. (c) The same as (b) but for different values of Λ with $\alpha = 15$ and $\epsilon_{\rm dd} = 10$.

$2\hbar^2 a/(ml_0^2)\delta(x)$, where $l_0 = \sqrt{\hbar/m\omega_\perp}$ and the DDI potential which takes the form [49,50]

$$V_d(x) = -g_d \frac{x^2 - 2\lambda^2}{(x^2+\lambda^2)^{5/2}}, \tag{3}$$

where $g_d = 2r_*/l_0$ with $r_* = md^2/\hbar^2$ being the characteristic dipole-dipole length. The potential $V_d(x)$ is repulsive for $x < \sqrt{2}\lambda$, while it is attractive at $x > \sqrt{2}\lambda$ which may open up the possibility of forming interwire polar molecules [see Fig. 2(a)]. The Fourier transform of the potential (3) reads $V_d(k) = g_d k^2[K_0(k\lambda) + K_2(k\lambda)]$, where $K_0(y)$ and $K_2(y)$ are modified Bessel functions [50]. For $k\lambda \ll 1$, the DDI potential reduces to $V_d(k) = g_d[2/\lambda^2 + \ln(2e^{-0.5-\gamma}/k\lambda)]$, where $\gamma = 0.5772$ is Euler's constant. In the frame of the Bogoliubov theory the Hamiltonian of the host reads

$$\hat{H}_B = \sum_{\mathbf{k}\neq 0} \hbar\omega_{\mathbf{k}} \hat{b}^\dagger_{\mathbf{k}} \hat{b}_{\mathbf{k}}, \tag{4}$$

where $\hat{b}^\dagger_{\mathbf{k}}$ and $\hat{b}_{\mathbf{k}}$ are operators of elementary excitations obeying the usual Bose commutation relations and the frequency of the Bogoliubov excitations is given by

$$\omega_q = \tfrac{1}{2}\omega_\perp \sqrt{q^4 + \alpha q^2\{1 + \epsilon_{\rm dd} q^2[K_0(q\Lambda) + K_2(q\Lambda)]\}}, \tag{5}$$

where $q = kl_0$ is the dimensionless wave vector, $\alpha = 8an$ is a dimensionless parameter depending on the condensate density n, $\Lambda = \lambda/l_0$ is the dimensionless interwire distance, and $\epsilon_{\rm dd} = g_d/g_{\rm 1D}$ is the relative strength describing the interplay between the DDI and contact interaction. For fixed interlayer separation and small $\epsilon_{\rm dd}$, the Bogoliubov spectrum (5) increases monotonically with q. As $\epsilon_{\rm dd}$ gets larger, ω_q exhibits first a maximum and then a minimum as the momentum increases results in roton-maxon structure as is seen in Fig. 2(b). If the roton minimum touches the zero-energy axis, the Bose condensate suffers a roton instability. The same behavior holds in quasi-2D dipolar BECs [51]. The energy and the height of the roton are sensitive to Λ as shown in Fig. 2(c). Note that a biwire system of polar molecules with dipole moments in the upper and lower wires, oriented in the same direction, cannot exhibit a roton-maxon character of the excitation spectrum.

For the sensor-reservoir (host-impurity) interaction we will assume, for simplicity, contact pseudopotential interaction potential, $V_{IB} = g_{IB}\delta(x)$, where $g_{IB} = 2\hbar^2 a_{IB}/m_{IB}(l_I^2 + l_0^2)$, and $m_{IB} = mm_I/(m + m_I)$ is the reduced mass. Although the sensor-reservoir coupling Hamiltonians are formally similar, they are substantially different due to the distinct trapping potentials of the impurity qubit. They are defined as [23]

$$H_{IB}^{\rm model\ I} = |e\rangle\langle e| \sum_{\mathbf{k}\neq 0} (\tilde{g}_{\mathbf{k}} \hat{b}_{\mathbf{k}} + \tilde{g}^*_{\mathbf{k}} \hat{b}^\dagger_{-\mathbf{k}}), \tag{6}$$

where the sensor-reservoir coupling parameter for model I is given

$$\tilde{g}_{\mathbf{k}} = g_{IB}\sqrt{\frac{n}{\ell}}\sqrt{\frac{\hbar^2k^2/2m}{\hbar\omega_{\mathbf{k}}}} \int d\mathbf{x}|\phi(\mathbf{x})|^2 e^{i\mathbf{kx}}, \tag{7}$$

and

$$H_{IB}^{\rm model\ II} = \sum_{\mathbf{k}\neq 0} \big[(\tilde{g}^r_{\mathbf{k}} \hat{b}_{\mathbf{k}} + \tilde{g}^{r*}_{\mathbf{k}} \hat{b}^\dagger_{-\mathbf{k}})(1+\sigma_z) + (\tilde{g}^l_{\mathbf{k}} \hat{b}_{\mathbf{k}} + \tilde{g}^{l*}_{\mathbf{k}} \hat{b}^\dagger_{-\mathbf{k}})(1-\sigma_z)\big], \tag{8}$$

where the sensor-reservoir coupling parameter for model II reads [19,23]

$$\tilde{g}^{r,l}_{\mathbf{k}} = g_{IB}\sqrt{\frac{n}{\ell}}\sqrt{\frac{\hbar^2k^2/2m}{\hbar\omega_{\mathbf{k}}}} \int d\mathbf{x}|\phi(\mathbf{x}_{r,l})|^2 e^{i\mathbf{kx}}, \tag{9}$$

where ϕ are the real eigenstates of impurity atoms localized in the internal state or the two wells of the potential U_I, and ℓ is the size of the quasi-1D condensate.

The total Hamiltonian of the system can be obtained by collecting three sub-Hamiltonian $H = H_I + H_B + H_{IB}$.

A. Dynamics of the qubit

The dynamics of the qubit in polar molecules reservoir is dephasing because H_I commutes with H_{IB}. More precisely, the diagonal elements of the density matrix are constant while the off-diagonal elements decay as $|\rho_I^{ij}(t)| = e^{-\Gamma(t)}\rho_I^{ij}(0)$, where $\rho_I^{ij} = \langle i|\rho_I|j\rangle$ and $i, j = r, l$ or e, g. The decoherence exponent Γ is defined for the two models as follows [19,23]:

$$\Gamma(t,T)^{\rm model\ I} = \sum_{\mathbf{k}} \frac{2g^2_{\mathbf{k}}}{\omega^2_{\mathbf{k}}} \sin^2\left(\frac{\omega_{\mathbf{k}}t}{2}\right) \coth\left(\frac{\omega_{\mathbf{k}}}{2k_BT}\right), \tag{10}$$

and

$$\Gamma(t,T)^{\text{model II}} = \sum_{\mathbf{k}} \frac{2g_{\mathbf{k}}^2}{\omega_{\mathbf{k}}^2} \sin^2\left(\frac{\omega_{\mathbf{k}} t}{2}\right) \sin^2(\mathbf{k}L) \times \coth\left(\frac{\omega_{\mathbf{k}}}{2k_B T}\right), \tag{11}$$

where the coupling parameters (7) and (9) turn out to be given as

$$g_{\mathbf{k}} = g_{IB}\sqrt{\frac{n}{\ell}}\sqrt{\frac{\hbar^2 k^2/2m}{\hbar\omega_{\mathbf{k}}}} e^{-(kl_I/2)^2}.$$

Note that the decoherence exponent Γ contains all the information concerning the time, the interaction, and temperature dependence of the decoherence process. For $\lambda \ll l_0$, one reproduces the results of Ref. [29] for impurity qubit immersed in a quasi-1D dipolar BEC. The thermal contribution $\coth[\omega_{\mathbf{k}}/(2k_B T)]$ to Γ originates from the normal and anomalous fluctuations of the condensate. If the dipolar BECs are at zero temperature, the decoherence factors (10) and (11) reduce to $\Gamma(t)^{\text{model I}} = \sum_{\mathbf{k}} (2g_{\mathbf{k}}^2/\omega_{\mathbf{k}}^2)\sin^2(\omega_{\mathbf{k}} t/2)$, and $\Gamma(t)^{\text{model II}} = \sum_{\mathbf{k}} (2g_{\mathbf{k}}^2/\omega_{\mathbf{k}}^2)\sin^2(\omega_{\mathbf{k}} t/2)\sin^2(\mathbf{k}L)$. In the short times limit, i.e., $\omega_{\mathbf{k}} t \ll 1$, one can approximate $\sin^2(\omega_{\mathbf{k}} t/2) \approx (\omega_{\mathbf{k}} t/2)^2$, thus, the decoherence factor is $\propto t^2$ for both models.

B. Non-Markovianity measure

Here, we check the existence of a Markovian-non-Markovian crossover and explain how the interwire separation affects the non-Markovianity of the reservoir. To this end, we follow the method proposed by Breuer *et al.* which is based on the dynamics of the so-called information flux $\sigma(t) = d\mathcal{D}[\rho_1(t), \rho_2(t)]/dt$ [52]. This represents the temporal change of two evolving quantum states, $\rho_{1,2}(t) = \Phi(t)\rho_{1,2}(0)$ as measured by the trace distance [22]. The non-Markovianity is defined to be the maximal amount of information that the system may recover from its environment, $\mathcal{N} = \max_{\rho_{1,2}(0)} \int_{\sigma>0} dt\sigma[t;\rho_{1,2}(0)]$. Frankly speaking, calculating $\mathcal{N}$ is a complicated task due to the difficult optimization over all pairs of initial states. However, for the purely dephasing system that is considered in this work, the trace distance between these two states takes the form $\mathcal{D}(t) = e^{-\Gamma(t)}$. This immediately gives the following expression of the non-Markovianity measure for a dephasing qubit [23,53]:

$$\mathcal{N} = \int_{\Gamma'(t)<0} \Gamma'(s) ds. \tag{12}$$

Equation (12) enables us to analyze effects of the background parameters such as the interwire separation, DDI, and temperature on the dynamics of information flow.

C. Temperature sensing

Now let us evaluate the temperature sensing precision of the qubit associated with state $\rho_l(t)$ of both models. The ultimate temperature sensing precision is restrained by the quantum Cramér-Rao bound, defined as $(\delta T)_{\min} = 1/\sqrt{\nu \mathcal{F}_T^Q}$ [54,55], where δT is the mean square error, ν is the number of repeated measurements, and

$$\mathcal{F}_T^Q = \frac{(\partial_T \Gamma)^2}{e^{2\Gamma} - 1},$$

accounts for the quantum Fisher information (QFI) with respect to the temperature T. Here Γ is the decoherence factor of both models. The temperature sensing performance can be characterized by the optimal relative error as [24]

$$\frac{(\delta T)_{\min}}{T} = \frac{1}{\sqrt{\nu Q_T}}, \tag{13}$$

where

$$Q_T = T^2 \mathcal{F}_T^Q, \tag{14}$$

denotes the QSNR. A higher QSNR indicates superior temperature sensing performance. As foreseen above, Q_T increases in a power law, t^α, at short times (see also Fig. 4). Obviously, Eqs. (10) to (14) demonstrate that the strength of the sensor-environment coupling and the interwire distance of the reservoir play a crucial role in the temperature measurement.

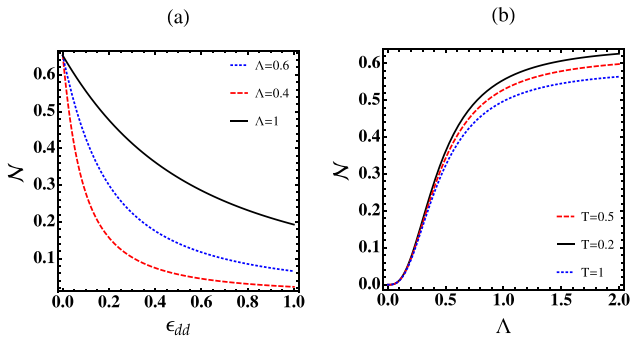

FIG. 3. (a) Non-Markovianity measure $\mathcal{N}$ for model I as a function as of the relative strength ϵ_{dd} for different values of the interwire distance Λ with $T = 0.2$. (b) Non-Markovianity as a function as of the interwire distance Λ for different values of temperature T with $\epsilon_{\text{dd}} = 0.1$. Parameters are $\tilde{l}_I = l_I/l_0 = 0.5$, and $\alpha = 4$.

III. NUMERICAL RESULTS

To be concrete, we consider a single ^{23}Na atom immersed in a polar molecule reservoir of KRb with a linear density is chosen to be $n = 5 \times 10^7 m^{-1}$. These molecules are characterized by a strong DDI which can be tuned using precisely controlled magnetic fields allowing atom pairs to be converted into weakly bound molecules known as Feshbach molecule [56]. The trapping frequency is assumed to be $\omega_\perp = 200$ Hz, and the corresponding oscillator length is $l_0 \simeq 1.5\,\mu$m.

A. Model I

Here we present the effects of the interwire space, the temperature and the DDI on the non-Markovianity, the QSNR, the maximum achievable QSNR, and the temperature optimal relative error of model I. Let us start by making a connection between the above decoherence factor and the non-Markovianity measure.

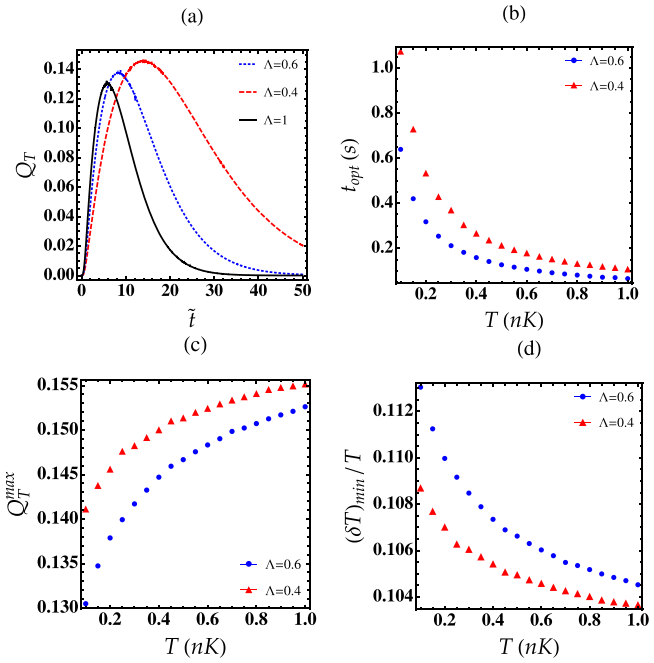

FIG. 4. (a) Dynamic behavior of the QSNR $Q_T(t)$ for model I as a function of time $\tilde{t} = \omega_T t$ for different interwire distance Λ. (b) Encoding time $t_{\rm opt}$ as a function of the temperature for two of Λ. (c) The maximum achievable QSNR, $Q_T^{\rm max}$ as a function of the temperature T for two values of Λ. (d) The optimal relative error $(\delta T)_{\rm min}/T$ for model I as a function of T from Eq. (13), after $\nu = 600$ measurements for two values of the interwire space, Λ. Parameters are $T = 0.2$ nK, $\tilde{l}_I = 0.5$, $\alpha = 4$, and $\epsilon_{\rm dd} = 0.1$. Here $\omega_T = k_B T/\hbar$.

Figure 3(a) depicts that the non-Markovianity, $\mathcal{N}$ decreases with the relative strength, $\epsilon_{\rm dd}$ for any Λ giving rise to reduce the fraction of recovered information flow.

Figure 3(b) shows that the interwire separation is crucial for the occurrence of non-Markovian reservoir memory effects. Particularly, for $\Lambda \lesssim 0.1$, $\mathcal{N}$ is negligible indicating that the polar molecule environment only receives information from the qubit (i.e., plays the role of emitter). However, increasing Λ amplifies the fraction of recovered information flow owing to the ability of the polar molecule to store and then supply information to the qubit. Another important remark is that the non-Markovianity, $\mathcal{N}$ decreases with temperature for $\Lambda \gtrsim 0.4$.

In Fig. 4(a) we plot the dynamical behavior of the QSNR for different interwire distances. We see that at short times $\tilde{t} \lesssim 5$, $Q_T(t)$ is higher for large Λ while the situation is reversed completely for long times $\tilde{t} > 5$. It develops a maximum with time where the position of such a maximum strongly depends on the interwire separation.

The maximum achievable QSNR $Q_T^{\rm max}$ can be evaluated by optimizing the encoding time $t_{\rm opt}$. Its behavior as a function of the temperature for different values of Λ is captured in Fig. 4(b). We observe that both $t_{\rm opt}$ and $Q_T^{\rm max}$ are increasing with decreasing Λ in the whole range of temperature T. Our numerical results show also that the maximum achievable QSNR rises monotonically with temperature for any Λ as seen in Fig. 4(c).

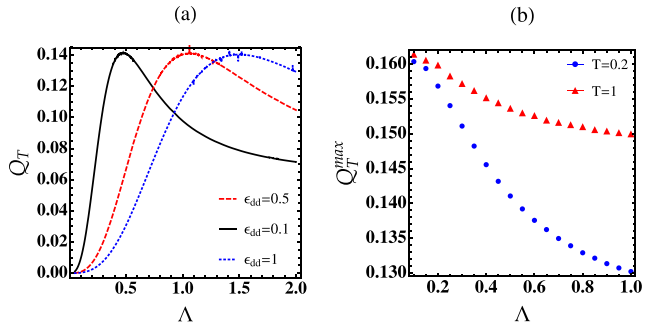

FIG. 5. (a) The QSNR Q_T for model I at the optimal point in time as a function of the interwire distance Λ for different values of $\epsilon_{\rm dd}$ and for $T = 0.2$ nK, $\tilde{l}_I = 0.5$, and $\alpha = 4$. (b) The maximum achievable QSNR $Q_T^{\rm max}(\Lambda)$ as a function of Λ for two values of temperature with $\epsilon_{\rm dd} = 0.1$.

Figure 4(d) depicts the optimal relative error $(\delta T)_{\rm min}/T$ as a function of temperature T after 600 measurements for two values of interwire space, Λ. We see that the optimal relative error varies slowly with temperature in the sub-nk regime, while it is sensitive to interwire space changes. For instance, for only 600 measurements $(\delta T)_{\rm min}/T \lesssim 11.3\%$ for $\Lambda = 0.6$ while it decays below 10.4% for $\Lambda = 0.4$ which is better than the sensing consisting of a qubit embedded into an ordinary BEC with short-range interactions [24]. One should stress that as the number of the measurements gets larger, the optimal relative error becomes marginal as shown in Eq. (13).

Figure 5(a) shows the optimal point in time for the variation of Q_T with Λ for different values of $\epsilon_{\rm dd}$. We see that Q_T first increases, reaches its maximum and then lowers with Λ notably for small relative DDI strength $\epsilon_{\rm dd}$. The hight and the width of the QSNR peak depend on Λ and on ϵ_{dd} giving rise to influence the temperature sensing performance. As can be seen from Fig. 5(b), the maximum achievable QSNR $Q_T^{\rm max}(\Lambda)$ is decreasing with the interwire space at any temperature.

B. Model II

In this section we calculate the above physical quantities in the frame of model II.

In Fig. 6 we show the non-Markovianity measure of model II versus the relative strength, $\epsilon_{\rm dd}$, and the interwire distance, Λ, for different values of the distance between two wells, $\tilde{L}$. We observe that when $\epsilon_{\rm dd}$ gets stronger, the non-Markovianity becomes very fragile notably for small Λ [see Fig. 6(a)]. A crossover from Markovian to non-Markovian dynamics occurs for large interwire space ($\Lambda \gtrsim 0.2$) as shown in Fig. 6(b). Such non-Markovianity becomes pronounced for larger $\tilde{L}$. Whereas for $\Lambda \lesssim 0.2$, the dynamics is Markovian for all the considered values of $\tilde{L}$. This reveals that to induce a non-Markovian dynamics, the interwire and inwerwell distances must be large enough to suppress effects of quantum and thermal fluctuations stemming from interactions.

Comparably with model I, Fig. 7(a) shows that the QSNR $Q_T(t)$ of model II reaches a maximum at time $t_{\rm opt}$, where the location of the peak relies on the interwire distance. For example, for $\Lambda = 1$ the peak is located at $t_{\rm opt} = 10$ while for $\Lambda = 0.4$, the maximum is attained at longer times, $t_{\rm opt} \simeq 25$.

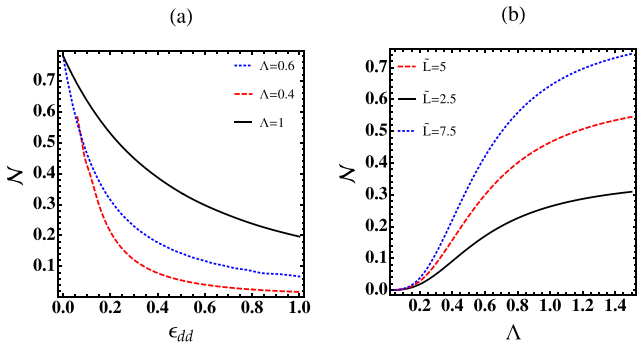

FIG. 6. (a) Non-Markovianity for model II as a function of the relative strength $\epsilon_{\rm dd}$ for different values of the interwire distance, Λ, with distance between two wells $\tilde{L} = L/l_0 = 7.5$. (b) Non-Markovianity as a function of Λ, for different values of $\tilde{L}$, and $\epsilon_{\rm dd} = 0.1$. Parameters are $T = 0.2$ nK, $\tilde{l}_I = 0.5$, $\alpha = 4$.

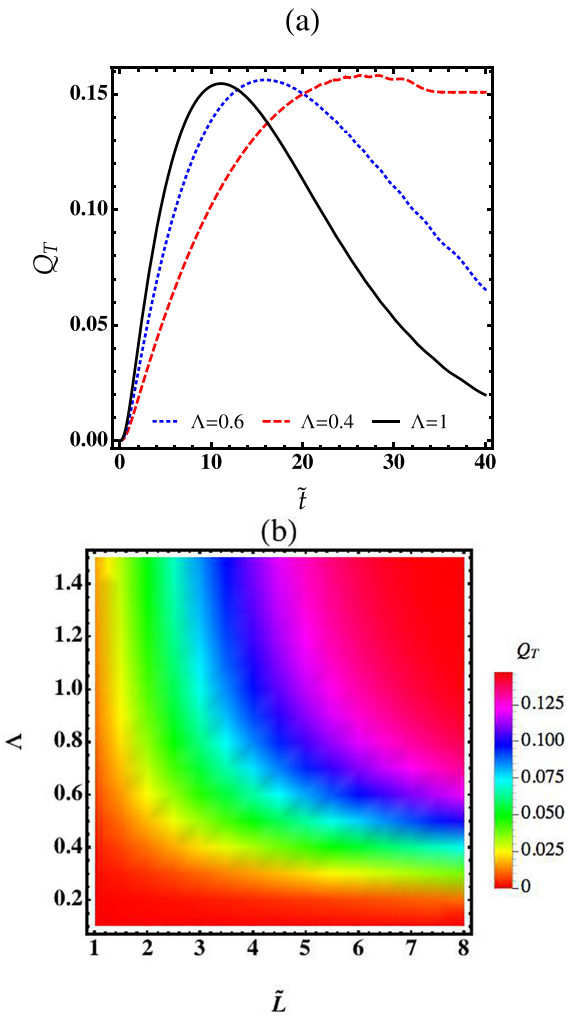

FIG. 7. (a) Dynamic behavior of the QSNR for model II as a function of time $\tilde{t}$ for different interwire distance Λ with $\tilde{L} = 7.5$. (b) The QSNR as a function of Λ and $\tilde{L}$ for $\tilde{t} \simeq 10$ and $T = 0.2$. Parameters are $\tilde{l}_I = 0.5$, $\alpha = 4$, and $\epsilon_{\rm dd} = 0.1$.

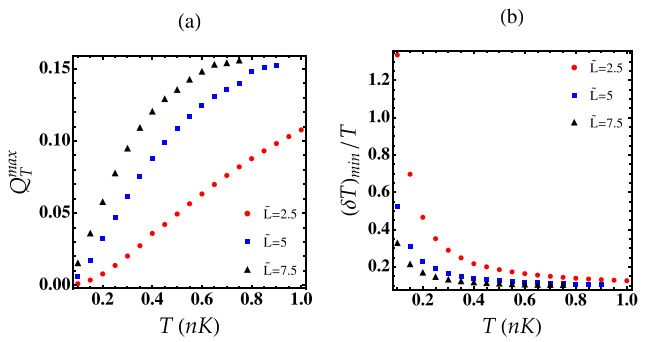

FIG. 8. (a) The maximum achievable QSNR for model II as a function of the temperature for three values of $\tilde{L}$. (b) The optimal relative error $(\delta T)_{\rm min}/T$ for model II as a function of temperature, T from Eq. (13), after $\nu = 600$ measurements for three values of $\tilde{L}$. Parameters are $T = 0.2$ nK, $\tilde{l}_I = 0.5$, $\alpha = 4$, and $\epsilon_{\rm dd} = 0.1$.

In Fig. 7(b) we plot the QSNR in plane $(\Lambda, \tilde{L})$ at time $\tilde{t} \simeq 10$ and temperature $T = 0.2$. We see that $Q_T(t)$ reaches its maximum for large Λ and $\tilde{L}$.

Similarly to the model I, the maximum achievable QSNR, $Q_T^{\rm max}$ of model II is increasing with T for any values of $\tilde{L}$ as shown in Fig. 8(a). We see also that $Q_T^{\rm max}$ rises with $\tilde{L}$.

According to the expression in Eq. (13), Fig. 8(b) shows that by adjusting the distance between two wells, the optimal relative error of the temperature is enhanced at any low temperature and for any interwire distance. For instance, for $\tilde{L} = 2.5$ one has $(\delta T)_{\rm min}/T \lesssim 12.6\%$ while it decreases to $\approx$10.3 for $\tilde{L} = 7.5$ which is comparable with the value found in model I. The obtained temperature sensing, which requires a wide interwell space $\tilde{L}$, clearly improves the results of [24] for sensing with an ordinary BEC.

IV. ROTONIZATION EFFECTS

Here we explore effects of rotonization on the dynamic behavior of the QSNR and on the non-Markovianity $\mathcal{N}$ for both models. It is clearly visible from Figs. 9(a) and 9(b) that in the presence of the roton-maxon in the reservoir spectrum, the QSNR $Q_T(t)$ of model I increases continuously with time inducing strong non-Markovian effects irrespective of the value of Λ. The absence of a peak in the QSNR indicates that the probe is not optimal for any temperature.

As shown in Fig. 9(c) the QSNR of model II saturates at a certain time in contrast to model I. The saturation time depends on the interwire distance. For large interwire distances, one can expect that $Q_T(t)$ saturates at long times. We see also that Q_T remains tiny during its time evolution signaling that the temperature sensing error will diverge as $T \to 0$ due to the rotonization effects. Figure 9(d) depicts the emergence of a non-Markovian dynamics of model II at $\Lambda \gtrsim 0.5$ for any $\tilde{L}$ indicating the existence of information backflows from the environment to the qubit.

By comparing the reduced dynamics of two different qubit models, we find that model II has higher values of the non-Markovianity measure than model I in agreement to the result of Ref. [23] for qubit models dephasing under the effect of an ordinary BEC state. Our results uncover also that the

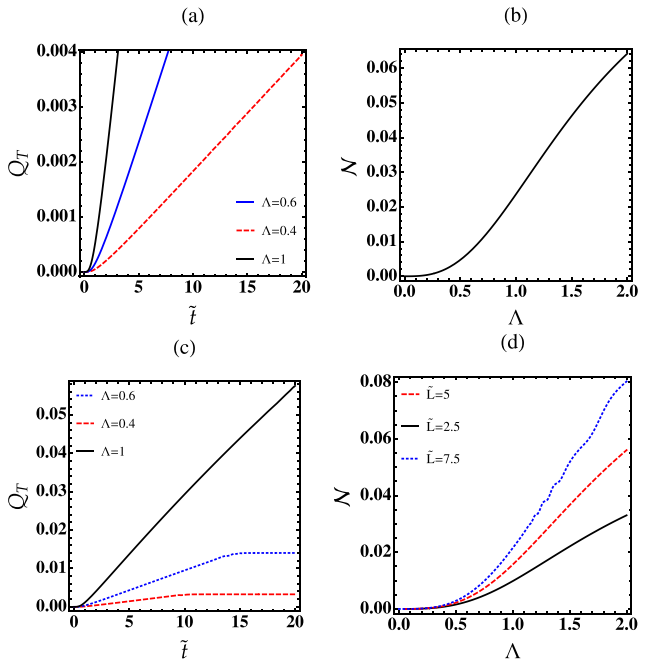

FIG. 9. (a) Dynamic behavior of $Q_T(t)$ for model I as a function of time $\tilde{t}$ for different interwire distance Λ. (b) Non-Markovianity, $\mathcal{N}$, for model I as a function as of Λ. (c) Dynamic behavior of $Q_T(t)$ for model II as a function of time $\tilde{t}$ for different values of Λ with $\tilde{L} = 7.5$. (d) Non-Markovianity for model II as a function of Λ for different values of $\tilde{L}$. Parameters are $T = 0.2$ nK, $\tilde{l}_l = 0.5$, $\alpha = 18$, and $\epsilon_{\rm dd} = 1$.

two models can have different sensitivity toward their polar molecules environment.

V. CONCLUSION

In this paper we proposed a quantum thermometer based on measurement of a mixed bosonic system consisting of two different models of an impurity qubit coupled to 1D biwire ultracold polar molecules where dipole moments are aligned head-to-tail across the wires. We found that the interwire separation plays a key role in the emergence of non-Markovian reservoir memory effects. By means of the QSNR, we studied numerically the temperature sensing performance and demonstrated that the interwire separation is indeed a relevant quantity for manipulating the information flowback and for enhancing the temperature sensitivity for both models. We revealed also that the rotonization strongly affects the QSNR and the thermometric performance of our models.

A comprehensive comparison of the two qubit models reveals that (i) the double-well model has larger values of the non-Markovianity measure than the intrinsic state structure in concordance with the results of Ref. [23] for qubit models dephasing under the effect of an ordinary BEC state, (ii) the two models have different sensitivity toward their polar molecules environment and different temperature optimal relative error, and (iii) a small value of the optimal relative error of temperature for a double-well qubit probe requires a wide interwell space and a large interwire distance.

Importantly, we showed that polar molecules are more appropriate than neutral atoms for enhancing the temperature sensitivity at extremely low temperatures. Our findings open up an avenue to the realization of quantum thermometers and of quantum simulators for non-Markovian open quantum systems with ultracold polar molecules.

ACKNOWLEDGMENTS

A.B. and K.A. acknowledge support from the Hassiba Benbouali University of Chlef. Q.-S.T acknowledges support from the National Natural Science Foundation of China (NSFC) (Grant No. 12275077) and the Natural Science Foundation of Hunan Province (Grant No. 2022JJ30277).

[1] C. L. Degen, F. Reinhard, and P. Cappellaro, Rev. Mod. Phys. **89**, 035002 (2017).
[2] D. Braun, G. Adesso, F. Benatti, R. Floreanini, U. Marzolino, M. W. Mitchell, and S. Pirandola, Rev. Mod. Phys. **90**, 035006 (2018).
[3] M. Mehboudi *et al.*, J. Phys. A: Math. Theor. **52**, 303001 (2019).
[4] P. Hauke, M. Heyl, L. Tagliacozzo, and P. Zoller, Nat. Phys. **12**, 778 (2016).
[5] I. Bloch, J. Dalibard, and S. Nascimbene, Nat. Phys. **8**, 267 (2012).
[6] H. Strobel *et al.*, Science **345**, 424 (2014).
[7] S. Chu, Rev. Mod. Phys. **70**, 685 (1998).
[8] C. N. Cohen-Tannoudji, Rev. Mod. Phys. **70**, 707 (1998).
[9] W. D. Phillips, Rev. Mod. Phys. **70**, 721 (1998).
[10] A. E. Leanhardt *et al.*, Science **301**, 1513 (2003).
[11] M. H. Anderson *et al.*, Science **269**, 198 (1995).
[12] K. B. Davis, M. O. Mewes, M. R. Andrews, N. J. van Druten, D. S. Durfee, D. M. Kurn, and W. Ketterle, Phys. Rev. Lett. **75**, 3969 (1995).
[13] B. De Marco and D. S. Jin, Science **285**, 1703 (1999).
[14] See for review: T. Lahaye *et al.*, Rep. Prog. Phys. **72**, 126401 (2009).
[15] K.-K. Ni, S. Ospelkaus, M. H. G. de Miranda, A. Peér, B. Neyenhuis, J. J. Zirbel, S. Kotochigova, P. S. Julienne, D. S. Jin, and J. Ye, Science **322**, 231 (2008).
[16] K. Aikawa, D. Akamatsu, M. Hayashi, K. Oasa, J. Kobayashi, P. Naidon, T. Kishimoto, M. Ueda, and S. Inouye, Phys. Rev. Lett. **105**, 203001 (2010).
[17] E. A. Cornell and C. E. Wieman, Rev. Mod. Phys. **74**, 875 (2002).
[18] A. Recati, P. O. Fedichev, W. Zwerger, J. von Delft, and P. Zoller, Phys. Rev. Lett. **94**, 040404 (2005).
[19] M. A. Cirone, G. De Chiara, G. M. Palma, and A. Recati, New J. Phys. **11**, 103055 (2009).
[20] Y. J. Song and L. M. Kuang, Ann. Phys. (Leipzig) **531**, 1800423 (2019).
[21] L. M. Kuang, H. S. Zeng, and Z. Y. Tong, Phys. Rev. A **60**, 3815 (1999).
[22] P. Haikka, S. McEndoo, G. De Chiara, G. M. Palma, and S. Maniscalco, Phys. Rev. A **84**, 031602(R) (2011).

[23] P. Haikka, S. McEndoo, and S. Maniscalco, Phys. Rev. A **87**, 012127 (2013).
[24] J.-B. Yuan, B. Zhang, Y.-J. Song, S.-Q. Tang, X.-W. Wang, and L.-M. Kuang, Phys. Rev. A **107**, 063317 (2023).
[25] D. Hangleiter, M. T. Mitchison, T. H. Johnson, M. Bruderer, M. B. Plenio, and D. Jaksch, Phys. Rev. A **91**, 013611 (2015).
[26] Q. Bouton, J. Nettersheim, D. Adam, F. Schmidt, D. Mayer, T. Lausch, E. Tiemann, and A. Widera, Phys. Rev. X **10**, 011018 (2020).
[27] W. Wu, S.-Y. Bai, and J.-H. An, Phys. Rev. A **103**, L010601 (2021); W. Wu, Z. Peng, S.-Y. Bai, and J.-H. An, Phys. Rev. Appl. **15**, 054042 (2021).
[28] J. B. Yuan, H. J. Xing, L. M. Kuang, and S. Yi, Phys. Rev. A **95**, 033610 (2017).
[29] L. Xu, J.-B. Yuan, S.-Q. Tang, W. Wu, Q.-S. Tan, and L.-M. Kuang, Phys. Rev. A **108**, 022608 (2023).
[30] V. Mukherjee, A. Zwick, A. Ghosh *et al.*, Commun. Phys. **2**, 162 (2019).
[31] Q-S. Tan, X. Liu, L. Xu, W. Wu, and L.-M. Kuang, Phys. Rev. A **109**, 042417 (2024).
[32] M. Brunelli, S. Olivares, and M. G. A. Paris, Phys. Rev. A **84**, 032105 (2011).
[33] M. Brunelli, S. Olivares, M. Paternostro, and M. G. A. Paris, Phys. Rev. A **86**, 012125 (2012).
[34] C. Sabín, A. White, L. Hackermuller, and I. Fuentes, Sci. Rep. **4**, 6436 (2014).
[35] S. Jevtic, D. Newman, T. Rudolph, and T. M. Stace, Phys. Rev. A **91**, 012331 (2015).
[36] L. Seveso and M. G. A. Paris, Phys. Rev. A **97**, 032129 (2018).
[37] A. H. Kiilerich, A. De Pasquale, and V. Giovannetti, Phys. Rev. A **98**, 042124 (2018).
[38] M. M. Feyles, L. Mancino, M. Sbroscia, I. Gianani, and M. Barbieri, Phys. Rev. A **99**, 062114 (2019).
[39] M. T. Mitchison, T. Fogarty, G. Guarnieri, S. Campbell, T. Busch, and J. Goold, Phys. Rev. Lett. **125**, 080402 (2020).
[40] A. Ullah, M. Tahir Naseem, and Ö. E. Müstecaplioglu, Phys. Rev. Res. **5**, 043184 (2023).
[41] M. Mehboudi, A. Lampo, C. Charalambous, L. A. Correa, M. A. Garcia-March, and M. Lewenstein, Phys. Rev. Lett. **122**, 030403 (2019).
[42] M. M. Khan, M. Mehboudi, H. Terças, M. Lewenstein, and M. A. Garcia-March, Phys. Rev. Res. **4**, 023191 (2022).
[43] M. M. Khan, H. Terças, J. T. Mendonça, J. Wehr, C. Charalambous, M. Lewenstein, and M. A. Garcia-March, Phys. Rev. A **103**, 023303 (2021).
[44] K. V. Hovhannisyan, M. R. Jørgensen, G. T. Landi, Á. M. Alhambra, J. B. Brask, and M. Perarnau-Llobet, PRX Quantum **2**, 020322 (2021).
[45] A. Boudjemâa, Phys. Lett. A **381**, 1745 (2017).
[46] A. Boudjemâa, J. Low. Temp. Phys. **189**, 76 (2017).
[47] M. Bruderer, A. Klein, S. R. Clark, and D. Jaksch, Phys. Rev. A **76**, 011605(R) (2007).
[48] H. T. Ng and S. Bose, Phys. Rev. A **78**, 023610 (2008).
[49] K. Łakomy, R. Nath, and L. Santos, Phys. Rev. A **86**, 013610 (2012).
[50] K. M. Elhadj, A. Boudjemâa and U. Al-Khawaja, Phys. Scr. **94**, 085402 (2019).
[51] A. Boudjemâa and G. V. Shlyapnikov, Phys. Rev. A **87**, 025601(R) (2013).
[52] H. P. Breuer, E. M. Laine, and J. Piilo, Phys. Rev. Lett. **103**, 210401 (2009).
[53] S.-Q. Tang, J.-B. Yuan, X.-W. Wang, and D.-Y. Zhang, J. Low. Temp. Phys. **189**, 147 (2017).
[54] C. W. Helstrom, *Quantum Detection and Estimation Theory* (Academic, New York, 1976).
[55] A. S. Holevo, *Probabilistic and Statistical Aspects of Quantum Theory* (North-Holland, Amsterdam, 1982).
[56] K.-K. Ni, S. Ospelkaus, D. J. Nesbitt, J. Ye, and D. S. Jin, Phys. Chem. Chem. Phys. **11**, 9626 (2009).